Contribution from Chemistry Department I (Inorganic Chemistry),
H. C. Orsted Institute, Universitetsparken 5, DK-2100 Copenhagen, Denmark

Electron Spin Resonance Spectra of Tetragonal Chromium(III) Complexes. I. *trans*-$[Cr(NH_3)_4XY]^{n+}$ and *trans*-$[Cr(py)_4XY]^{n+}$ in Frozen Solutions and Powders. A Correlation between Zero-Field Splittings and Ligand Field Parameters *via* Complete d-Electron Calculations

ERIK PEDERSEN*[1] and HANS TOFTLUND

Received November 28, 1973 AIC30864S

The frozen-solution X-band esr spectra have been recorded for complexes of the type *trans*-$[Cr(NH_3)_4XY]^{n+}$ with the XY combinations FF, ClCl, BrBr, FBr, F(H_2O), Br(H_2O), (H_2O)(H_2O), (OH)(OH), Br(ONO), and (NCS)(NCS) and for the type *trans*-$[Cr(py)_4XY]^{n+}$ with the XY combinations FF, ClCl, BrBr, II, FCl, FBr, F(H_2O), Cl(H_2O), Br(H_2O), F(OH), Cl(OH), (H_2O)(H_2O), and (OH)(OH). Complexes with only halide or pseudohalide ligands all show tetragonal symmetry with $1.97 \leq g \leq 1.99$ and zero-field splittings $0.30 \leq 2D \leq 3.5$ cm^{-1}. Complexes with the ligands H_2O and OH^- have rhombic symmetry. X- and Q-band spectra have been recorded for some of the halide complexes as powders diluted in the corresponding cobalt(III) or rhodium(III) complexes. These have approximately the same g and D values as the frozen solutions but show rhombic distortions corresponding to $0 \leq E \leq 0.04$ cm^{-1}. The zero-field splittings have been correlated with theoretical calculations based on all 120 states of the d^3 configuration and semiempirical parameters previously determined from vis-uv absorption spectra. Assuming the free-ion value of the spin-orbit coupling constant, these calculations show satisfactory agreement with the experimental values for complexes with nonheavy ligands. Second-order perturbation calculations including the lowest quartet and doublet states are inadequate.

Introduction

There have already been performed many correlations between the esr spectra of the ground states and the vis-uv spectra of the nearest excited states in transition metal complexes. Most of such work is, however, unsatisfactory because of an unfavorable number of parameters involved, compared to the number of observables. Many of the systems that have been studied have shown such a low symmetry that it has been impossible to extract from the vis-uv spectra the interelectronic repulsion parameters and all the ligand field parameters, required by symmetry. Except for the calculations of the zero-field splittings of the ground states in ruby[2-4] and for other preliminary calculations [5-8] computational difficulties for systems with more than one unpaired electron have necessitated crude approximations, neglecting most of the excited states.

It was the purpose of the present investigation to attempt to solve these problems by studying the esr spectra of simple systems, having a well-characterized high symmetry. Two almost ideal series of chromium(III) complexes of the types *trans*-$[Cr(NH_3)_4XY]^{n+}$ and *trans*-$[Cr(py)_4XY]^{n+}$ are now available through the work of Glerup and Schaffer.[9,10] Within the framework of the angular overlap model the ligand field and interelectronic repulsion parameters are rather well known, at least to an accuracy sufficient for a good description of the transitions between quartet states.[10,11] Carrying out complete calculations involving repulsion, ligand field, spin-orbit coupling, and Zeeman effect within the d^3 configuration was feasible in tetragonal symmetry.[12] These calculations with or without Zeeman effect required diagonalizations of energy matrices of the orders 120 and 30, respectively. Only the results of the zero-field calculations will be mentioned here.

Experimental Section

Preparation of Complexes. All chromium complexes have kindly been placed at our disposal by J. Glerup. Details of the preparation of some of the ammonia complexes have already been published.[9] The procedures for the preparation of the pyridine complexes will be published later.[10] As the solid solvents for the magnetic dilution of the chromium complexes have great influence on the rhombic distortions from tetragonal symmetry we give details of the preparation of these.

trans-**Dichlorotetraamminerhodium(III) nitrate** was prepared by precipitation with 4 *M* nitric acid from an aqueous solution of the chloride, prepared according to Johnson and Basolo.[13]

trans-**Dichlorotetrakis(pyridine)rhodium(III) chloride hexahydrate** was prepared by Delepine.[14] We used one of his original samples after recrystallization from hot water.

trans-**Dibromotetrakis(pyridine)rhodium(III) Bromide Hexahydrate.** We tried repeatedly but unsuccessfully to prepare samples of this complex according to the literature method.[15] All such samples contained large and irreproducible amounts of chloride, partly coordinated to rhodium. We therefore modified the procedure, mainly by using a large excess of bromide. Two grams of rhodium(III) chloride trihydrate (7.6 mmol) and 10 g of lithium bromide (0.12 mol) dissolved in 16 ml of water were boiled for 10 min with formation of $[RhBr_6]^{3-}$. The brown solution was quickly cooled in ice to 40°, and 8 ml of pyridine (0.1 mol) was added. The mixture was quickly heated over a flame to 70° (heating too slowly gives a brown nonreacting and unidentified precipitate) followed by the addition of 5 drops of a 50% w/w aqueous solution of hypophosphoric acid. Further heating nearly to boiling gave an orange solution and a heavy brown-orange precipitate. The hot solution was filtered and the filtrate left overnight in a refrigerator (3°). The orange-yellow crystals which formed were washed with ice water and recrystallized from water by heating to 95° and then cooling to 3°. The first formed precipitate appeared as very thin plates. By leaving these in the mother liquor at 3° for 2 days they recrystallized into compact monoclinic crystals with a size suitable for X-ray studies. The results of

(1) To whom correspondence should be addressed at the Department of Chemistry, Texas A&M University, College Station, Tex. 77843.

(2) R. M. Macfarlane, *J. Chem. Phys.*, 39, 3118 (1963).
(3) R. M. Macfarlane, *J. Chem. Phys.*, 42, 442 (1965).
(4) R. M. Macfarlane, *J. Chem. Phys.*, 47, 2066 (1967).
(5) D. T. Sviridov and R. K. Sviridova, *Kristallografiya*, 14, 920 (1969).
(6) D. T. Sviridov and Yu. F. Smirnov, *Spektrosk. Tverd. Tela*, 258 (1969); *Chem. Abstr.*, 72, 94880 (1970).
(7) Z. Rudzikas and A. Jucys, *Liet. Fiz. Rinkinys*, 9, 533 (1969).
(8) F. Cariati, A. Sgamellotti, and V. Valenti, *Atti Acad. Naz. Lincei, Cl. Sci. Fis., Mat. Natur., Rend.*, 45, 344 (1968).
(9) J. Glerup and C. E. Schaffer, *Chem. Commun.*, 38 (1968).
(10) J. Glerup, private communication.
(11) J. Glerup and C. E. Schaffer, *Proc. Int. Conf. Coord. Chem.*, 11, 500 (1968).
(12) S. E. Harnung, O. Monsted, and E. Pedersen, to be submitted for publication.
(13) S. A. Johnson and F. Basolo, *Inorg. Chem.*, 1, 925 (1962).
(14) M. Delepine, *Bull. Soc. Chim. Fr.*, [4] 45, 235 (1929).
(15) J. A. Osborn, R. D. Gillard, and G. Wilkinson, *J. Chem. Soc.*, 3168 (1964).

the microanalyses of C, H, N, and Br agreed within 0.5% with the values calculated for the formula $[Rh(C_5H_5N)_4Br_2]Br\cdot 6H_2O$. The water and rhodium contents were determined by means of the thermobalance described previously.[16] An 18.70-mg sample was heated at a rate of 5° min^{-1} in static air with a relative humidity of 35% at 25°. A 14.2% portion was lost between 58 and 123° after which the sample retained constant weight up to 200°. The calculated water content is 14.10%. After decomposition in several steps the sample had a constant weight from 640 to 900°, where the heating was stopped. The residue corresponded to 16.6%. The calculated value for Rh_2O_3 is 16.55%. Only a trace of chloride was detectable in the bromide.

Esr Spectra. The X-band spectra were recorded on a JEOL JES-ME-1X spectrometer. The magnetic field range is 20–7300 G (2×10^{-3}–0.73 T). The frequency was measured with a resonant cavity wavemeter to an accuracy of 1 MHz. The field calibration below 2000 G was performed with a Hall probe gaussmeter with an accuracy of 1 G. Above 2000 G a sample of oxygen at 0.7 Torr was used as a reference having very narrow peaks at small intervals throughout the whole field range. The positions and frequency dependencies of these have been carefully measured by Tinkham and Strandberg.[17] The accuracy of the field measurements in this range is thus determined by the wavemeter. The Q-band spectra were kindly recorded by JEOL in Tokyo on powdered samples at room temperature on a JES-ME-3Q instrument in the field range 4000–14000 G. The accuracy of frequency and field in these recordings is 0.5%.

Mixtures of water, dimethylformamide, and methanol in the volume ratios 1:1:2, ethanol and methanol in the volume ratio 5:1, or glycerol and water in the volume ratio 1:1 were used as solvents for the frozen solutions. The pyridine complexes were measured at concentrations from 10^{-2} to 10^{-4} *M*. They are soluble in all three solvents as chlorides, bromides, and perchlorates. The ammonia complex salts with these anions were completely insoluble in the alcohol mixture. In the two other solvents we used the concentrations 10^{-3}–10^{-4} *M*. The frozen-solution spectra were recorded at −150°. Procedures were carefully controlled so that no crystallization took place. In contrast to earlier experience[18] we observed in some cases considerable molecular motion even at −120°. Normal 5-mm sample tubes were suitable because of the low dielectric loss in the frozen state.

Unless specifically mentioned all spectra were recorded by using a 100-kHz modulation field with amplitudes between 5 and 20 G. These spectra therefore appear as first derivatives of the absorptions. Second-derivative spectra were obtained by simultaneously modulating with an 80-Hz field.

The frozen-solution spectra of salts with different anions in different solvents were recorded. Small variations in the line widths were observed, but the spin-Hamiltonian parameters were almost identical. Only one spectrum of each complex will be shown in Figures 1–6.

Interpretation of the Spectra

The esr spectra of all the complexes investigated could be accurately described in terms of the conventional spin-Hamiltonian operator

$$\mathcal{H} = g_{\parallel}\beta H_z S_z + g_{\perp}\beta(H_x S_x + H_y S_y) + D[S_z^2 - {}^1/_3 S(S+1)] + E(S_x^2 - S_y^2) \quad (1)$$

for $S = {}^3/_2$. The shapes of the random orientation spectra and general diagrams for fitting of the spin-Hamiltonian parameters are discussed in the Appendix. Our measurements do not give the sign of the zero-field splitting (hereafter called zfs) which in the axially symmetric case is given by zfs = $2D$ with the states described by $M_s = \pm {}^1/_2$ being the Kramers doublet with lowest energy in the absence of a magnetic field. As discussed later, we do, however, expect all the complexes to have positive D values. Measurements at temperatures where $kT \approx 2D$ might confirm this. As it has been discussed previously in the literature[19] there is an arbitrary choice in naming the axes x, y, and z. However,

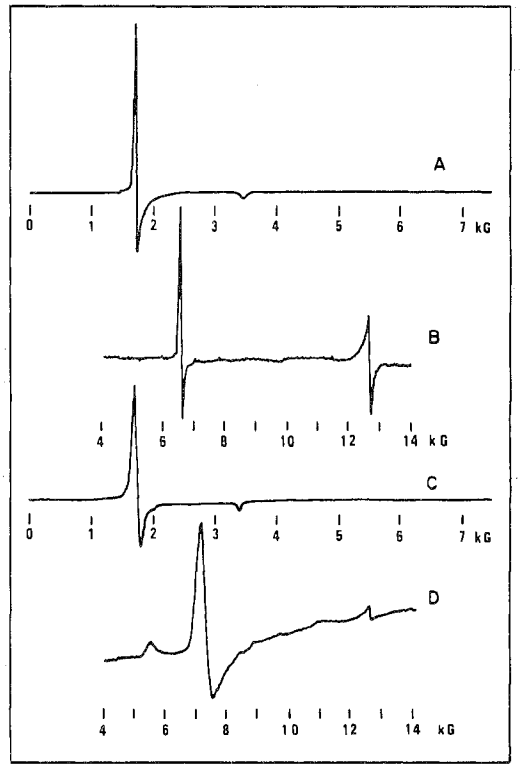

Figure 1. Esr spectra: A, *trans*-$[Cr(py)_4I_2]^+$ in DMF–H_2O–MeOH glass at 9.30 GHz; B, *trans*-$[Cr(py)_4I_2]^+$ in *trans*-$[Rh(py)_4Br_2]Br\cdot 6H_2O$ powder at 35.4 GHz; C, *trans*-$[Cr(py)_4Br_2]^+$ in DMF–H_2O–MeOH glass at 9.30 GHz; D, *trans*-$[Cr(py)_4Br_2]^+$ in *trans*-$[Rh(py)_4Br_2]Br\cdot 6H_2O$ powder at 35.4 GHz.

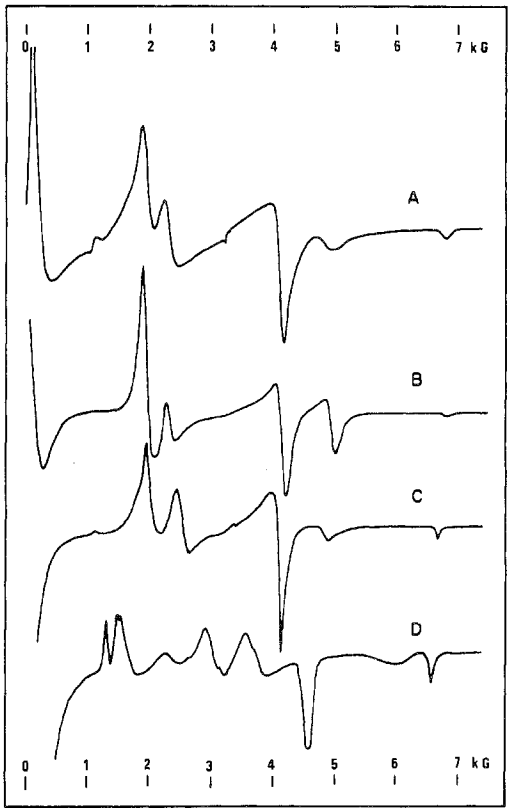

Figure 2. Esr spectra: A, *trans*-$[Cr(py)_4Cl_2]^+$ in DMF–H_2O–MeOH glass at 9.211 GHz; B, computer-simulated spectrum with $g_{\parallel} = g_{\perp} = 1.99$, $D = 0.164$ cm^{-1}, $E = 0$, and single molecule lorentzian line widths of 200 G; C, *trans*-$[Cr(py)_4Cl_2]^+$ in *trans*-$[Rh(py)_4Cl_2]Cl\cdot 6H_2O$ powder at 9.447 GHz; D, *trans*-$[Cr(py)_4Cl_2]^+$ in *trans*-$[Rh(py)_4Br_2]Br\cdot 6H_2O$ powder at 9.447 GHz.

(16) E. Pedersen, *J. Sci. Instrum.*, [2] 1, 1013 (1968).
(17) M. Tinkham and M. W. P. Strandberg, *Phys. Rev.*, 97, 951 (1955).
(18) J. C. Hempel, L. O. Morgan, and W. B. Lewis, *Inorg. Chem.*, 9, 2064 (1970).
(19) L. L. van Reijen, Thesis, Technische Hogeschool, Eindhoven, The Netherlands, 1964.

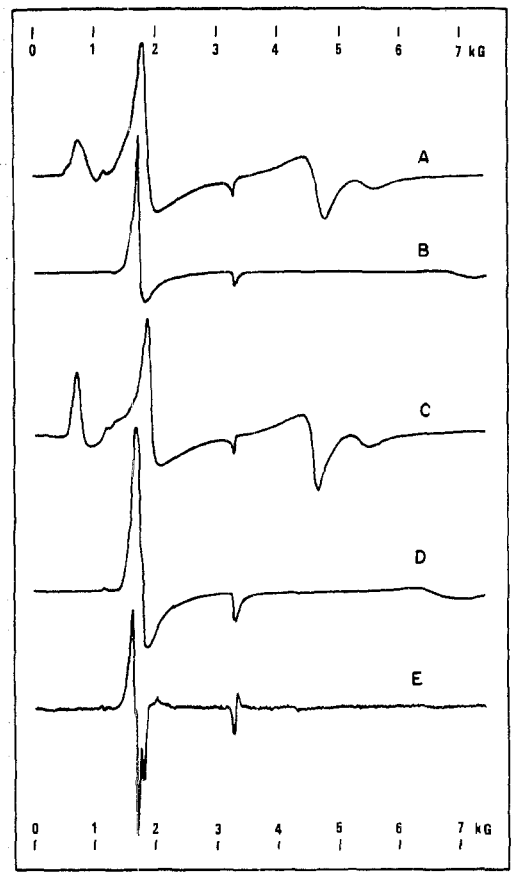

Figure 3. Esr spectra: A, *trans*-$[Cr(py)_4F_2]^+$ in DMF-H_2O-MeOH glass at 9.217 GHz; B, *trans*-$[Cr(py)_4FBr]^+$ in DMF-H_2O-MeOH glass at 9.216 GHz; C, *trans*-$[Cr(py)_4FCl]^+$ in DMF-H_2O-MeOH glass at 9.210 GHz; D, *trans*-$[Cr(py)_4Br(H_2O)]^{2+}$ in DMF-H_2O-MeOH glass at 9.215 GHz; E, second derivative of Figure 3D.

only one choice leads to $0 \leq 3E \leq D$. The esr spectra of the axially symmetric complexes in frozen solutions do not tell whether the magnetic fourfold symmetry axes are perpendicular to the plane containing the four nitrogen ligators. This is assumed, however, and the arguments are presented later in this paper.

A detailed discussion of the interpretation of all the spectra will not be given. The general procedure has been to locate prominent peaks or points of inflection, corresponding to x, y, z, or intermediate orientations of the static magnetic field relative to the molecular magnetic axes by means of the graphs in Figures 15-17 in the Appendix. Thereby good estimates of the spin-Hamiltonian parameters could be obtained in all cases. Detailed computer simulations based on these preliminary parameters were then performed, followed by small adjustments of the parameters. It is essential to realize that the presence of some very intense peaks in the spectra cannot be explained and that accurate spin-Hamiltonian parameters cannot be obtained without a complete computer simulation of the spectra. One example of the method of interpretation follows. The D and E parameters are given in Tables I and II. The g tensors were found to be almost isotropic. Because of line widths of 50 G or more these are not very accurately determined. The principal values were all in the range 1.97-1.99. The anisotropies were less than 0.01. The g tensors and their variation will not be discussed in this paper.

Example of Parameter Fitting. The X-band spectrum of *trans*-$[Cr(py)_4Cl(H_2O)]^{2+}$ as a frozen solution in DMF-H_2O-MeOH, recorded at 9.209 GHz, is shown in Figure 4A. The

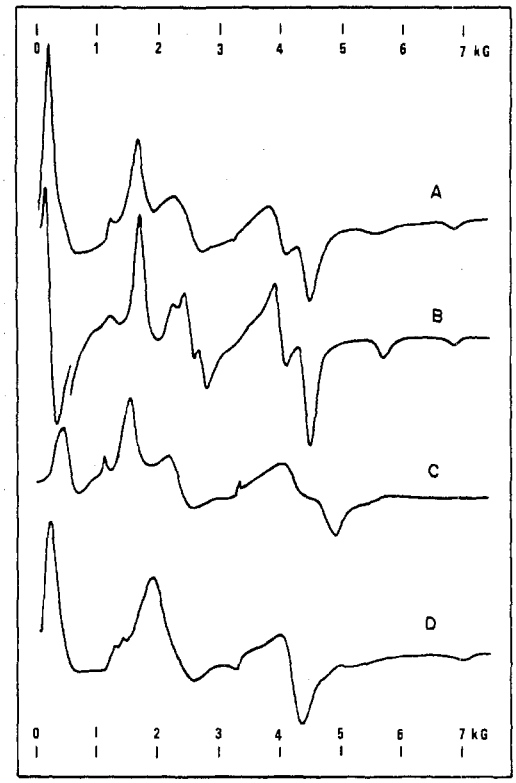

Figure 4. Esr spectra: A, *trans*-$[Cr(py)_4Cl(H_2O)]^{2+}$ in DMF-H_2O-MeOH glass at 9.209 GHz; B, computer-simulated spectrum with $g_\parallel = g_\perp = 1.99$, $D = 0.160$ cm^{-1}, $E = 0.02$ cm^{-1}, and single molecule lorentzian line widths of 200 G; C, *trans*-$[Cr(py)_4F(H_2O)]^{2+}$ in DMF-H_2O-MeOH glass at 9.251 GHz; D, *trans*-$[Cr(py)_4(H_2O)_2]^{3+}$ in DMF-H_2O-MeOH glass 1 M in perchloric acid at 9.210 GHz.

solution was 0.1 M in perchloric acid. The approximate value of the zero-field splitting zfs $= 2\sqrt{D^2 + 3E^2} \approx h\nu$ is obvious from the position of the intense band at low field. The weak $-1/2 \rightarrow 1/2$ z transition at 3300 ±25 G gives $g_\parallel = 1.99$. The $-3/2 \rightarrow 1/2$ z transition at 6800 ± 50 G determines the value of $|D| = 0.160 \pm 0.002$ cm^{-1}, independent of E. Assuming $g_\perp = g_\parallel$ this is in agreement with the position of the intermediate orientation bands. The splitting of these into the component in the zx plane at 3950 ± 25 G and the component in the yz plane at 4450 ± 25 G gives $E = 0.020 \pm 0.002$ cm^{-1}. These parameters now explain the position of the y transition at 5650 ± 50 G and the apparent absence of the corresponding x transition because of overlap with the intermediate orientation band in the yz plane. The broad band with a point of inflection at 2450 G is required to be a superposition of two x and one y transitions. The point of inflection of the y transition at 1700 ± G and the "zero-field transitions" at 150 ± 25 G confirm the values of the first assumed parameters. Note that the $-3/2 \rightarrow 3/2$ z transition has gained intensity and moved slightly upfield relative to the spectra of complexes with $E = 0$. The computer-simulated spectrum, assuming the previously mentioned parameters and individual lorentzian line widths of 200 G, is shown in Figure 4B

Calculations of Zero-Field Splittings

The calculation of zero-field splittings of the ground states in transition metal complexes is normally performed using second-order perturbation theory,[20] including the nearest states with the same spin multiplicity as the ground states. For complexes with an orbitally nondegenerate ground state

(20) B. R. McGarvey, *Transition Metal Chem.*, 3, 89 (1966).

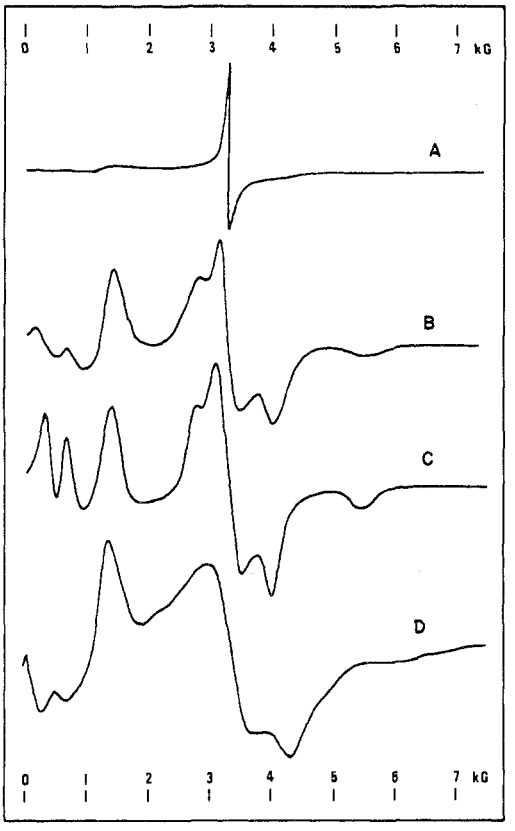

Figure 5. Esr spectra: A, *trans*-$[Cr(py)_4(OH)_2]^+$ in DMF-H_2O-MeOH glass 0.1 *M* in OH^- at 9.215 GHz; B, *trans*-$[Cr(py)_4Cl(OH)]^+$ in DMF-H_2O-MeOH glass 0.1 *M* in OH^- at 9.216 GHz; C, computer-simulated spectrum with $g_x = g_y = g_z = 1.99$, $D = 0.105$ cm^{-1}, $E = 0.03$ cm^{-1}, and single molecule lorentzian line widths of 250 G; D, *trans*-$[Cr(py)_4F(OH)]^+$ in DMF-H_2O-MeOH glass 0.1 *M* in OH^- at 9.20 GHz.

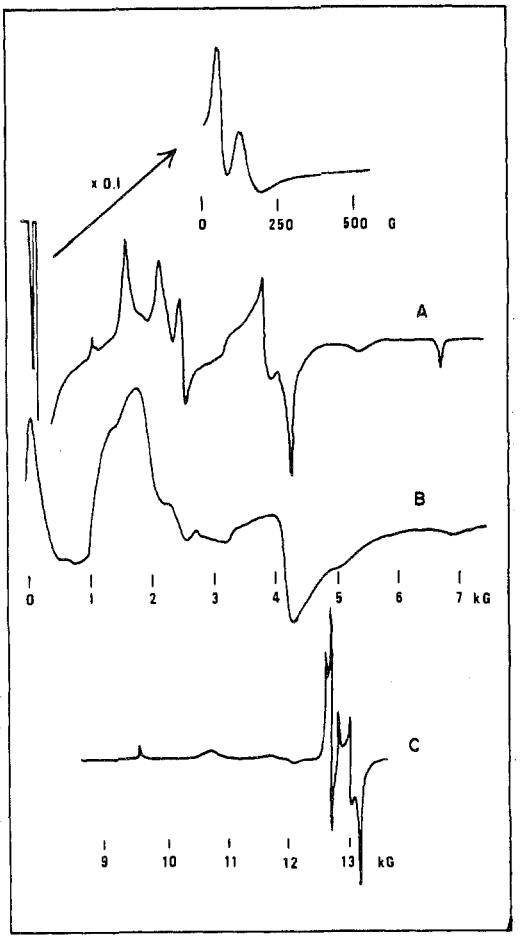

Figure 6. Esr spectra: A, *trans*-$[Cr(NH_3)_4Cl_2]^+$ in *trans*-$[Rh(NH_3)_4Cl_2]NO_3$ powder at 9.185 GHz; B, *trans*-$[Cr(NH_3)_4Cl_2]^+$ in DMF-H_2O-MeOH glass at 9.250 GHz; C, *trans*-$[Cr(NH_3)_4Cl_2]^+$ in *trans*-$[Rh(NH_3)_4Cl_2]NO_3$ powder at 35.5 GHz.

the spin-orbit coupling or a low-symmetry ligand field may mix the ground state with the excited states, thus giving rise to zfs. The influence of the low-symmetry field is sometimes referred to as configuration interaction. This treatment, neglecting many of the excited states and couplings between these, requires that zfs is approximately a linear function of the orbital splittings of the excited states included in the calculation. These orbital splittings are determined mainly by the ligand field. A d^3 system as Cr(III) with a $^4A_{2g}$ ground state in octahedral symmetry and all the excited states more than approximately 15 kK away is expected to be one of those which follows the predictions of the second-order theory most accurately. For Cr(III) in an axial ligand field Van Vleck[21] thus calculated the zfs according to

$$2D = E|\pm 3/2\rangle - E|\pm 1/2\rangle = {}^8/_9\zeta^2 \frac{E(^4A) - E(^4E)}{\Delta^2} \qquad (2)$$

where ζ is the one-electron spin-orbit coupling constant (ζ = 273 cm^{-1} for the gaseous Cr^{3+} ion), $E(^4A)$ and $E(^4E)$ are the energies of the trigonal components ^4A and ^4E of the octahedral $^4T_2$ states, and Δ is the average one-electron energy difference between the e and t_2 orbitals (for $\zeta = 0$ Δ equals the energy of the $^4T_2$ states in octahedral symmetry). This calculation includes only second-order spin-orbit coupling effects, and for trigonal symmetry it neglects the far more important configuration interaction between $^4A_2$ states. Later treatments[22-25] have considered this interaction and spin-orbit coupling interactions with the doublet states. Macfarlane's complete calculations within the d^3 configuration[2-4] gave satisfactory results for zfs of the ground states in ruby. There seems to be an error in Macfarlane's spin-orbit coupling matrices. This is of minor importance for the ground states, however, and this problem will be deferred to a later discussion.[12]

For tetragonal symmetry eq 2 has been considered a good approximation. The importance of charge-transfer states has been estimated.[26] The inclusion of these states has otherwise mostly been confined to the calculation of *g* factors.[27-29]

We felt that it was necessary to control the approximations made in simple perturbation calculations within the d^3 configuration before the introduction of more sophisticated effects such as electron delocalization and orbital reduction factors,[30] interaction with charge-transfer states,[26] anisotropic spin-orbit coupling,[25] etc. Through the work of Harnung[12] the complete interelectronic repulsion, ligand field, and spin-

(21) J. H. Van Vleck, *J. Chem. Phys.*, 7, 61 (1939).
(22) P. H. E. Meijer and H. J. Gerritsen, *Phys. Rev.*, 100, 742 (1955).
(23) S. Sugano and M. Peter, *Phys. Rev.*, 122, 381 (1961).
(24) L. L. Lohr, Jr., and W. N. Lipscomb, *J. Chem. Phys.*, 38, 1607 (1963).
(25) H. Kamimura, *Phys. Rev.*, 128, 1077 (1962).
(26) B. B. Garrett, K. DeArmond, and H. S. Gutowsky, *J. Chem. Phys.*, 44, 3393 (1966).
(27) R. Lacroix and G. Emch, *Helv. Phys. Acta*, 35, 592 (1962).
(28) R. Lacroix, *C. R. Acad. Sci.*, 252, 1768 (1961).
(29) A. A. Misetich and T. Buch, *J. Chem. Phys.*, 41, 2524 (1964).
(30) M. Gerloch and J. R. Miller, *Progr. Inorg. Chem.*, 10, 1 (1968).

Table I. Zero-Field Splitting Parameters of Pyridine Complexes (cm^{-1})

Complex	Medium	Freq	$\|D\|$	$\|E\|$
trans-$[Cr(py)_4I_2]^+$	DMF-H_2O-MeOH	X	>0.4	<0.01
	trans-$[Rh(py)_4Br_2]Br\cdot 6H_2O$	X	>0.4	<0.01
		Q	1.75 ± 0.25	<0.01
trans-$[Cr(py)_4Br_2]^+$	DMF-H_2O-MeOH	X	>0.4	<0.01
	trans-$[Rh(py)_4Br_2]Br\cdot 6H_2O$	X	>0.4	<0.01
		Q	0.710 ± 0.005	0.010 ± 0.002
trans-$[Cr(py)_4Cl_2]^+$	DMF-H_2O-MeOH	X	0.164 ± 0.002	<0.001
	trans-$[Rh(py)_4Cl_2]Cl\cdot 6H_2O$	X	0.157 ± 0.002	<0.001
	trans-$[Rh(py)_4Br_2]Br\cdot 6H_2O$	X	0.150 ± 0.005	0.04 ± 0.01
trans-$[Cr(py)_4F_2]^+$ [b]	DMF-H_2O-MeOH	X	0.226 ± 0.004	<0.001
trans-$[Cr(py)_4FBr]^+$		X	0.49 ± 0.02	<0.002
trans-$[Cr(py)_4FCl]^+$		X	0.215 ± 0.004	<0.001
trans-$[Cr(py)_4Br(H_2O)]^{2+}$	DMF-H_2O-MeOH, 0.1 *M* H^+	X	0.45 ± 0.02	0.010 ± 0.002
trans-$[Cr(py)_4Cl(H_2O)]^{2+}$		X	0.160 ± 0.002	0.020 ± 0.002
trans-$[Cr(py)_4F(H_2O)]^{2+}$		X	0.185 ± 0.002	0.020 ± 0.002
trans-$[Cr(py)_4(H_2O)_2]^{3+}$	DMF-H_2O-MeOH, 1 *M* H^+	X	0.165 ± 0.002	0.008 ± 0.002
trans-$[Cr(py)_4(OH)_2]^+$ [a]	DMF-H_2O-MeOH, 0.1 *M* OH^-	X	<0.01	<0.003
trans-$[Cr(py)_4Cl(OH)]^+$		X	0.105 ± 0.001	0.030 ± 0.001
trans-$[Cr(py)_4F(OH)]^+$		X	0.12 ± 0.01	0.030 ± 0.005

[a] This complex is very labile, especially in strongly basic solution. The solution was made by dissolving the diaqua complex at room temperature in the DMF-H_2O-MeOH mixture, made slightly acidic by addition of perchloric acid. Excess base was added at −50°. This procedure avoided dissociation of pyridine as shown by addition of excess perchloric acid, giving the usual diaquo spectrum without detectable impurities. [b] The esr spectrum of this complex shows a strong medium dependence. This is also observed in the vis-uv spectra and may be ascribed to hydrogen-bonding phenomena. This problem may account for the poor agreement with the theoretical calculations. Rapid precipitation with perchloric acid from aqueous solutions containing 0.2–3% of this complex relative to the corresponding cobalt(III) complex gave crystalline powders with very small Cr:Co ratios and having very complicated esr spectra with more than 30 lines. Slower crystallizations from water containing 5% of chromium relative to cobalt yielded large crystals without a trace of chromium.

Table II. Zero-Field Splitting Parameters of Ammonia Complexes (cm^{-1})

Complex	Medium	Freq	$\|D\|$	$\|E\|$
trans-$[Cr(NH_3)_4Br_2]^+$	DMF-H_2O-MeOH	X	>0.4	<0.01
trans-$[Cr(NH_3)_4Cl_2]^+$		X	0.160 ± 0.003	<0.002
	trans-$[Rh(NH_3)_4Cl_2]NO_3$	X	0.157 ± 0.001	0.0150 ± 0.0005
		Q	0.156 ± 0.001	0.0152 ± 0.0005
trans-$[Cr(NH_3)_4F_2]^+$	DMF-H_2O-MeOH	X	0.254 ± 0.008	<0.005
trans-$[Cr(NH_3)_4FBr]^+$		X	0.47 ± 0.01	<0.005
trans-$[Cr(NH_3)_4F(H_2O)]^{2+}$	DMF-H_2O-MeOH, 0.1 *M* H^+	X	0.24 ± 0.01	<0.02
trans-$[Cr(NH_3)_4(H_2O)_2]^{3+}$	DMF-H_2O-MeOH, 0.5 *M* H^+	X	0.17 ± 0.01	<0.005
trans-$[Cr(NH_3)_4(OH)_2]^+$	DMF-H_2O-MeOH, 0.1 *M* OH^-	X	<0.01	<0.003
trans-$[Cr(NH_3)_4(NCS)_2]^+$	DMF-H_2O-MeOH	X	0.25 ± 0.01	<0.01
trans-$[Cr(NH_3)_4Br(ONO)]^+$		X	0.120 ± 0.005	<0.01

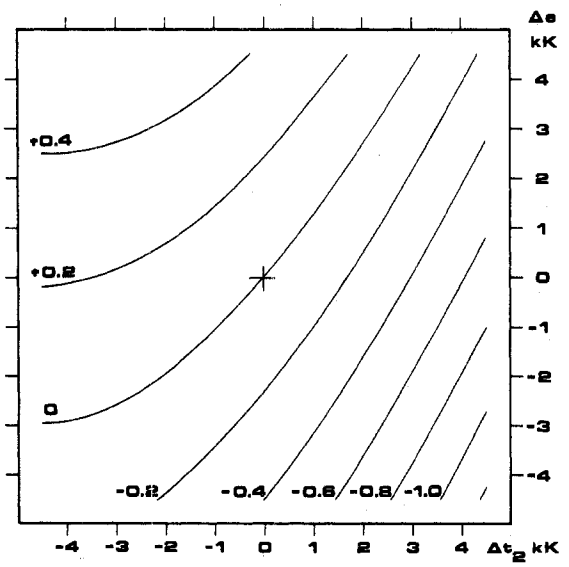

Figure 7. Calculated zero-field splittings ($2D$) in units of cm^{-1} for tetragonal d^3 systems, based on complete calculations within the d^3 configuration. The variation of zfs as a function of the tetragonal ligand field parameters Δe and Δt_2 for fixed values of the other parameters: $\Delta_{av} = 19{,}500$, $B = 600$, $C = 3000$, $\zeta = 273$ cm^{-1}.

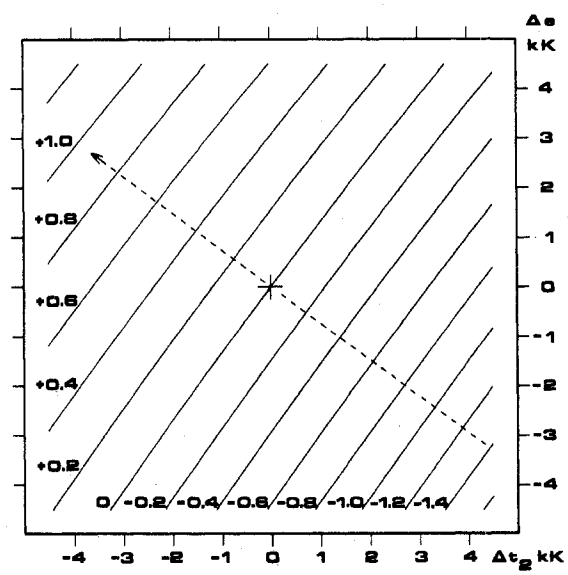

Figure 8. Calculated zero-field splittings ($2D$) in units of cm^{-1} for tetragonal d^3 systems, based on calculations within all quartet states of the d^3 configuration. The same set of parameters is used as in Figure 7. The dashed axis gives the variation of the diagonal ligand field splitting of the octahedral $^4T_2$.

orbit coupling matrices for d^3 in D_4 and D_3 symmetry were available. They were derived by tensor methods and therefore in a weak-field formalism. In D_4 the 120 states of d^3 decompose into 30 Γ_6 and 30 Γ_7 states, each doubly degenerate in the absence of a magnetic field. The calculation of zfs, that is the energy difference between the lowest Γ_6 and

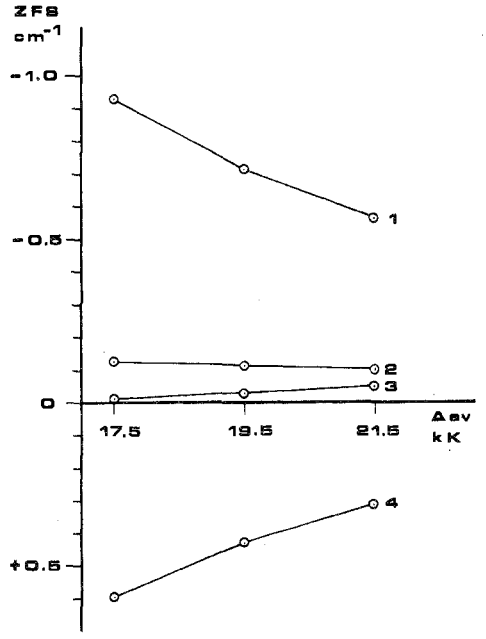

Figure 9. Complete calculations of zero-field splittings as functions of Δ_{av}; $B = 600$, $C = 3000$, $\zeta = 273$: (1) $\Delta e = -3000$, $\Delta t_2 = 3000$; (2) $\Delta e = 3000$, $\Delta t_2 = 3000$; (3) $\Delta e = -3000$, $\Delta t_2 = -3000$, (4) $\Delta e = 3000$, $\Delta t_2 = -3000$ (all in cm^{-1}).

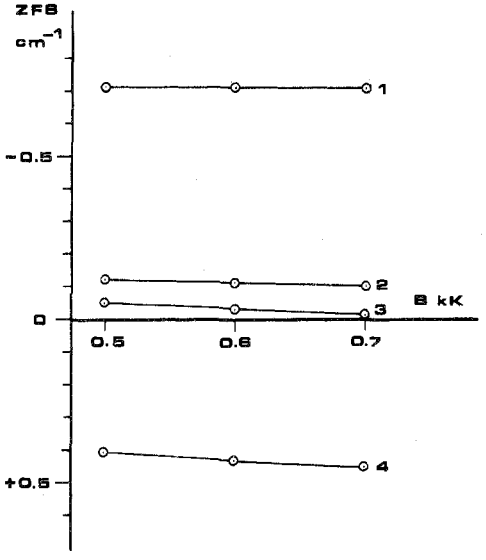

Figure 10. Complete calculations of zero-field splittings as functions of the Racah parameter B; $\Delta_{av} = 19{,}500$, $C = 3000$, $\zeta = 273$ cm^{-1}. The numbers refer to the same set of parameters as in Figure 9.

Γ_7, thus requires diagonalizations of matrices of the size 30 × 30. Spin-orbit coupling mixes $^4A_2(t_2^3)$ with the excited states $^4T_2(t_2^2e)$, $^2T_2(t_2^3)$, $^2T_2'(t_2^2e)$, and $^2T_2''(t_2^2e)$, arranged in order of increasing energy of these states. All direct interactions give contributions to the zfs, because all four levels show orbital splittings in D_4. The t_2^2e levels have diagonal ligand field splittings. The $^2T_2(t_2^3)$ level is split only through the interaction with $^2E(t_2^3)$ with lower energy. The nondiagonal matrix element is Δt_2.[11] This splitting is normally small but can be very important. An example is *trans*-$[Cr(NH_3)_4F_2]^+$ with very large Δt_2 where the splitting is 1.4 kK. The $^4T_2$ splitting is 2.8 kK.[11] The baricenter of $^4T_2$ has the approximate energy Δ_{av}. The octahedral $^2T_2(t_2^3)$ has the diagonal strong-field energy $5(3B + C)$. In most complexes mentioned here it is close to the components of $^4T_2$.

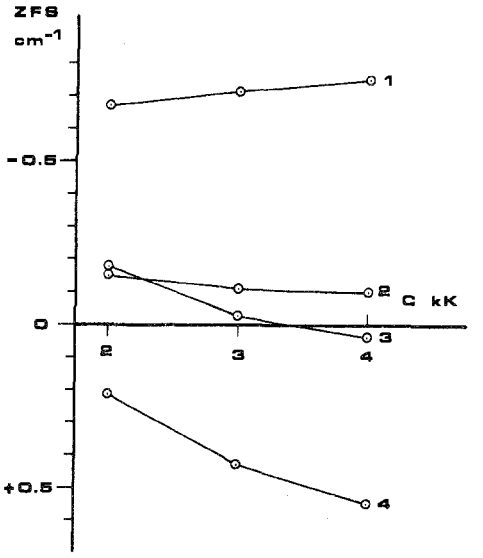

Figure 11. Complete calculations of zero-field splittings as functions of the Racah parameter C; $\Delta_{av} = 19{,}500$, $B = 600$, $\zeta = 273$ cm^{-1}. The numbers refer to the same set of parameters as in Figure 9.

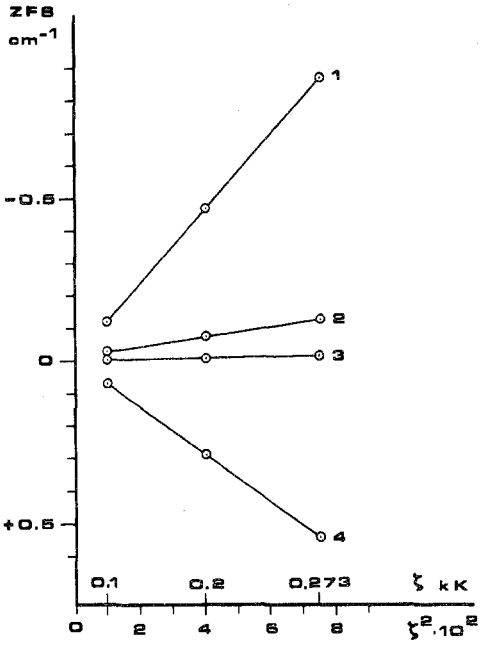

Figure 12. Complete calculations of zero-field splittings as functions of ζ^2; $\Delta_{av} = 18{,}000$, $B = 600$, $C = 3000$ cm^{-1}. The numbers refer to the same set of parameters as in Figure 9.

The diagonal ligand field splitting of $^4T_2$ into ^4E and $^4B_2$ in D_4 is

$$E|^4B_2\rangle - E|^4E\rangle = {}^3/_4\Delta e - \Delta t_2 \qquad (3)$$

This is the only important ligand field parameter together with Δ_{av} and ζ in Van Vleck's simplified calculations, eq 2.

It seems an insuperable task to illustrate the complete seven-dimensional space, containing the zfs and the parameters Δ_{av}, Δe, Δt_2, B, C, and ζ, included in our calculations. However, all the important features are evident from simple two- or three-dimensional projections, Figures 7-12. In Figure 7 is shown the dependence of Δe and Δt_2 for $\Delta_{av} = 19.5$ kK, $B = 0.6$ kK, $C = 3.0$ kK, and $\zeta = 0.273$ kK. These parameters are average values for the whole series of complexes. This projection clearly illustrates the need of two independent tetragonal ligand field parameters. The results of a similar calculation, but neglecting the doublet states, are

Table III. Theoretical Zero-Field Splittings, Calculated from the Free-Ion Value of ζ and Parameters Obtained from Vis-Uv Absorption Spectra[a]

Complex	Δ_{av}	Δe	Δt_2	B	C	ζ	Zfs	ζ_{exptl}
trans-$[CrN_4(OH)_2]^+$	20,300	−3500	−4500	675	3375	273	0.023	270
trans-$[CrN_4(H_2O)_2]^{3+}$	19,500	1500	−2000	675	3375	273	0.305	280
trans-$[CrN_4F_2]^+$	19,900	−1000	−3500	706	3530	273	0.196	420
trans-$[CrN_4Cl_2]^+$	18,800	3000	−2000	603	3015	273	0.435	240
trans-$[CrN_4Br_2]^+$	18,700	4500	−1000	600	3000	273	0.511	450
trans-$[CrN_4I_2]^+$	18,400	5500	−500	586	2930	273	0.583	640

[a] The "experimental" spin-orbit coupling constant ζ_{exptl} must be applied in order to obtain agreement with the experimental zfs values. Based on crudely estimated uncertainties of the spectral parameters we estimate the uncertainties of the theoretical zfs values to be 25% or 0.02 cm^{-1}, whichever is greater. All units are in cm^{-1}; zfs = $2D$.

Table IV. Partial Derivatives of Zfs for the Parameter Values in Table III

Complex	$10^5\partial zfs/\partial\Delta_{av}$	$10^5\partial zfs/\partial\Delta e$	$10^5\partial zfs/\partial\Delta t_2$	$10^5\partial zfs/\partial B$	$10^5\partial zfs/\partial C$	$10^3\partial zfs/\partial\zeta$
trans-$[CrN_4(OH)_2]^+$	−2.0	6.0	−2.3	21	−13	0
trans-$[CrN_4(H_2O)_2]^{3+}$	−4.5	8.0	−6.5	8.3	6.6	2.3
trans-$[CrN_4F_2]^+$	−3.5	8.0	−5.0	13	7.3	1.4
trans-$[CrN_4Cl_2]^+$	−6.0	9.0	−5.5	13	9.1	3.4
trans-$[CrN_4Br_2]^+$	−7.0	9.5	−9.0	8.3	7.1	4.0
trans-$[CrN_4I_2]^+$	−8.0	10	−10	8.0	7.5	4.6

shown in Figure 8. Here it is obvious that all values of Δe and Δt_2 obeying the relation

$$\Delta e = 1.3\Delta t_2 + \text{constant} \quad (4)$$

give constant zfs. The effective parameter is thus $(\Delta e/1.3) - \Delta t_2$. This is equal to the diagonal ligand field splitting of $^4T_2$. In the complete calculations, Figure 7, this is obviously not a good parameter. As it has been argued for trigonal complexes,[24] it might be assumed that the addition of contributions to zfs from $^2T_2(t_2^3)$ would make a considerable improvement to the quartet model. We isolated the contributions of all doublets from the t_2^3 configuration ($^2T_2$, $^2T_1$, ^2E) by setting $\Delta_{av} = 5 \times 10^6$ kK with the other parameters unchanged. This gives the diagonal doublet energies $n(3B + C)$ where $n = 3$ for ^2E and $^2T_1$ and $n = 5$ for $^2T_2$. The maximum zfs value within the $\Delta e - \Delta t_2$ range shown in Figures 7 and 8 was 0.07 cm^{-1}, independent of Δe as expected. The sum of the contributions from $^4T_2$ and the lowest doublets is thus very far from approximating zfs obtained from complete calculations. The variations with the other parameters are illustrated in Figures 9-12. Zfs shows what is believed to be an accidental independence of B. The dependence of C, large C giving large zfs, reveals once again the influence of the doublets, the energies of the quartet states being independent of C. The dependence of Δ_{av} was that expected, large Δ_{av} giving small zfs. Zfs is approximately proportional to ζ^2, as shown in Figure 12. This is reasonable because all matrix elements between the ground states and the excited states are proportional to ζ. Qualitatively the same dependence of the parameters are observed for all values of the parameters being reasonable for chromium(III) complexes. Interpolations from Figures 7-12 can be performed with good accuracy.

Within the weak-field scheme used in the calculations the eigenvectors do not directly tell which of the excited strong-field states are the most important in a second-order perturbation language. A future discussion based on transformations to a strong-field scheme will settle this question. We can, however, conclude that zfs consists of several partly canceling contributions from both quartet and doublet states.

In Table III are given the results of our calculations for each complex of the type *trans*-$[CrN_4X_2]^{n+}$ where N refers to the nitrogen ligating atoms. ζ is not known experimentally for any of these or similar complexes. We therefore tentatively used the free-ion value. Δ_{av}, Δe, Δt_2, and B have been obtained by Glerup and Schaffer[10,11] from gaussian analyses of the vis-uv quartet transition spectra of the ammonia complexes. For the difluoro complex C was derived from the positions of the lowest doublets $^2E(t_2^3)$ and $^2T_1(t_2^3)$. In other cases we assumed $C = 5B$. The vis-uv spectra of the pyridine complexes are similar to those of the corresponding ammonia complexes. We therefore assumed the same parameters for both series. The parameters will probably undergo small changes when fitted to the larger experimental material now available.[10] The differentials of the theoretical zfs values with respect to all parameters are therefore included in Table IV.

Discussion of the Measurements

Symmetry. Our experimental material falls into two classes: frozen solutions and polycrystalline powders. The complexes generally show the highest symmetry in frozen solutions. Here complexes with linear trans ligators (halides) all have tetragonal symmetry within the uncertainty determined by the line widths of the esr spectra. Aquo and hydroxo complexes have rhombic symmetry as expected for nonlinear ligators under circumstances where the rotational freedom is hindered. Complexes with a single water or hydroxo ligand have the highest degree of rhombic distortion. We take this as an experimental indication that two coordinated molecules trans to each other prefer a noneclipsed conformation. Rhombic splittings from water molecules as ligands in solution have previously been discussed by Schaffer.[31] He noticed that the vis-uv absorption spectra of the hexaaqua ions of transition metal complexes show stronger temperature dependence of the line widths and the positions than complexes with linear ligators.

Almost all complexes studied in polycrystalline powders show varying rhombic distortions, depending of the anions and the lattice in general. *trans*-$[Rh(py)_4Br_2]Br\cdot 6H_2O$, for example, crystallizes in the space group $P2_1/c$.[32] No tetragonal sites are therefore available, and *trans*-$[Cr(py)_4Cl_2]^+$ in this lattice has a strong rhombic distortion.

The line widths of the powder spectra are considerably narrower than those of the frozen-solution spectra. This may be due to random fluctuations of the ligand positions in the frozen solutions as also indicated by a comparison between experimental and computer-simulated spectra. Single molecule line widths of 20 G or less may account for the

(31) C. E. Schaffer, *Struct. Bonding (Berlin)*, 5, 68 (1968).
(32) S. Yde-Andersen, K. J. Watson, and E. Pedersen, to be submitted for publication.

line widths of the powder spectra. It is, however, impossible to obtain simulated spectra completely identical with the glass spectra by assuming equal line widths for all individual orientations. This will make the z transitions $-3/2 \rightarrow 3/2$ and $-1/2 \rightarrow 1/2$ too broad relative to the other transitions. These are the only ones in the spectra which are completely independent of both D and E. A typical example is the glass spectrum of *trans*-$[Cr(py)_4Cl(H_2O)]^{2+}$, Figure 4A, compared with the simulated spectrum, Figure 4B, with single molecule line widths of 200 G. In the simulated spectrum the three lines between 2000 and 2700 G (those having positions most sensitive to D and E) are too narrow compared with Figure 4A, whereas the $-3/2 \rightarrow 3/2$ transition is too broad.

Correlations with Theory. Before a closer examination of the agreement between experimental and theoretical zfs values we will discuss the presence of other contributions to zfs than those considered in our calculations. One of these is the interaction with the lowest charge-transfer states, having energies comparable to or smaller than the highest energy states of the d^3 configuration. One attempt to estimate this contribution has been made,[26] but we feel that the present experimental and theoretical knowledge of these charge-transfer states is so poor that they cannot be included in a quantitative calculation. Of less importance is the dipolar spin-spin interaction.[33-35] Another entirely experimental problem in the study of magnetic properties of molecules is the overwhelming importance of small deviations from the anticipated symmetry. In the investigations of single-crystal[33] and frozen-solution[18] esr spectra of *trans*-bis(ethylenediamine)chromium(III) complexes it was thus found that the carbon chains were of much greater importance for the magnitude of zfs than were the tetragonal distortions due to the trans ligands, dominating the splittings in the vis-uv spectra. This was explained by McGarvey[33] in terms of configuration interaction *via* the rhombic ligand field between the ground states and one of the orbital components of $^4T_1(t_2{}^2e)$, both transforming as $^4B_1$ in D_{2h} symmetry.

This low-symmetry problem seems to be absent for the two series of complexes studied here. All dihalide complexes have tetragonal symmetry in frozen solutions. They have approximately the same zfs in powders, even in the presence of small rhombic lattice distortions. Single-crystal esr spectra[36] and the X-ray structure[32] of the *trans*-dibromotetrakis(pyridine)chromium(III) complex diluted in the corresponding rhodium(III) complex as a bromide hexahydrate show that the magnetic fourfold axes coincide with the molecular Br-Br axes. For aqua and hydroxo complexes in frozen solution the rhombic contributions to zfs are small compared to the tetragonal contributions. We feel that this set of arguments justifies a correlation between the experimental zfs values and the results of calculations in tetragonal symmetry.

In a second-order perturbation calculation where the tetragonal splitting of the $^4T_2$ level is the most important contribution to zfs, one can expect zfs to vary according to the positions of the trans ligands in the spectrochemical series (A) $I^- > Br^- > Cl^- > H_2O > F^- > OH^-$. This series corresponds to a decreasing diagonal ligand field splitting of the $^4T_2$ level. The complete calculations clearly show the individual importance of Δe and Δt_2, and deviations from the above series could be expected. The theoretical zfs values in Table III happen to vary according to series A, although the numerical values are far from those predicted by the quartet model in eq 2. The experimental results in Tables I and II give the series (B) $I^- >> Br^- >> F^- > Cl^- \simeq H_2O >> OH^-$, in agreement with series A except for fluoro complexes. As mentioned in footnote *b* of Table I fluoro complexes have esr spectra showing a very complicated dependence of the surrounding medium, not alone related to hydrogen-bonding phenomena. Some systems have very many lines. We cannot explain this. Complexes of the type *trans*-$[CrN_4XY]^{n+}$ always have zfs values between those of *trans*-$[CrN_4X_2]^{n+}$ and *trans*-$[CrN_4Y_2]^{n+}$ as predicted.

Except for the iodo and bromo complexes the zfs values obtained from the complete calculations by assuming the free-ion value of the spin-orbit coupling constant are in satisfactory agreement with the experimental values. As shown in Table III $\zeta > 273$ cm^{-1} must be assumed for iodo and bromo complexes. There is other experimental evidence for this. Linhard and Weigel[37] found very large intensities of the spin-forbidden $^4A_2 \rightarrow {}^2T_2(t_2{}^3)$ (O symmetry) transitions in the vis-uv spectra of $[Cr(NH_3)_5Br]^{2+}$ and $[Cr(NH_3)_5I]^{2+}$. Glerup[10] also observed this transition to be very intense and well separated from the quartet transitions in *trans*-$[Cr(py)_4Br_2]^+$ and *trans*-$[Cr(py)_4I_2]^+$. The intensity can be explained by spin-orbit coupling interaction between these doublet states and the nearest quartet states.[38] The intensity will thus be proportional to ζ^2 and inversly proportional to the square of the energy separation to the nearest quartet. An estimate of ζ in bromo and iodo complexes obtained in this way agrees qualitatively with the values in Table III. Within a MO calculation including the lowest quartet states,[26] increased zfs values are expected in complexes with such heavy ligands because of the large spin-orbit coupling effects in these atoms, not necessarily because of large MO coefficients indicating pronounced covalency.

In simplified calculations, including the lowest quartet and doublet states, the approximate cubic magnetic symmetry of the ground states in *trans*-dihydroxo complexes can only be explained by assuming $\zeta = 0$. This physically unreasonable assumption is avoided in the complete calculation within the d^3 configuration.

Acknowledgments. We are grateful to J. Glerup for his permission to use many of his samples and to him and C. E. Schaffer for valuable inspiration during this work. We are also indebted to S. E. Harnung and O. Monsted for the permission to use their computer programs and to P. Trinderup for important contributions to the computer programs for simulation of esr spectra.

Appendix

Computer Simulation of Random Orientation Esr Spectra. At an early stage of this investigation it became evident that the spectra could not be interpreted in terms of x, y, and z transitions only. We therefore performed a computer simulation based on the spin Hamiltonian, eq 1.

The eigenfunctions $|\nu_k\rangle$ with eigenvalues λ_k are expanded in terms of the complete set $|m_s\rangle$

$$|\nu_k\rangle = \sum_{m_s} |m_s\rangle\langle m_s|\nu_k\rangle \qquad (5)$$

(33) B. R. McGarvey, *J. Chem. Phys.*, 41, 3743 (1964).
(34) R. M. Pitzer, C. W. Kern, and W. N. Lipscomb, *J. Chem. Phys.*, 37, 267 (1962).
(35) J. S. Griffith in "The Theory of Transition Metal Ions," Cambridge University Press, London, 1961, p 330.
(36) S. Yde-Andersen and E. Pedersen, to be submitted for publication.
(37) M. Linhard and M. Weigel, *Z. Anorg. Allg. Chem.*, 266, 49 (1951).
(38) C. K. Jorgensen, *Acta Chem. Scand.*, 9, 1362 (1955).

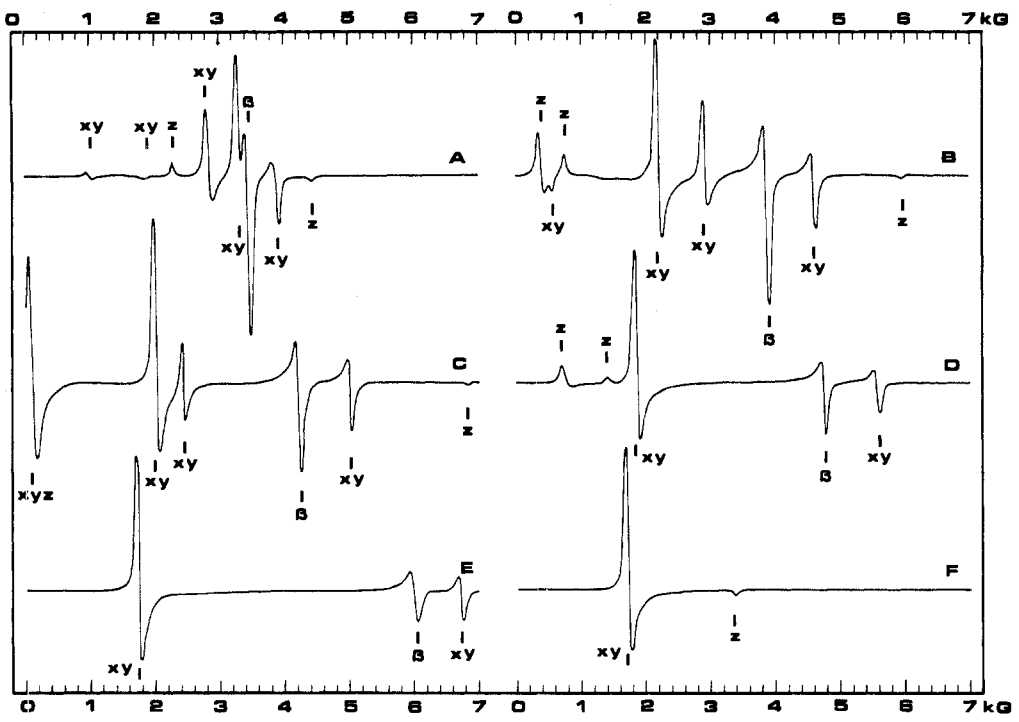

Figure 13. Computer-simulated random orientation spectra with $g_x = g_y = g_z = 1.98$, $E = 0$, $h\nu = 0.31$ cm^{-1}: (A) $D = 0.05$; (B) $D = 0.12$; (C) $D = 0.16$; (D) $D = 0.22$; (E) $D = 0.35$; (F) $D = 0.70$ cm^{-1}. Single molecule spectra with lorentzian line widths of 100 G were added for every step of 0.5° in the polar angle Θ. β refers to intermediate orientation lines.

In matrix notation the eigenvalue problem is

$$\mathbf{HU} = \mathbf{U}\Lambda \tag{6}$$

where **H** is a 4 × 4 matrix with the elements $\langle m_s|H|m_s'\rangle$, Λ is a diagonal matrix with the elements λ_k, and **U** is a unitary matrix with $\langle m_s|\nu_k\rangle$ as components of the column vectors. **H** is generally hermitian, but real symmetric for $H_y = 0$. The numerical diagonalization performed according to the Jacobi procedure for real symmetric matrices required the transcription of eq 7 giving the eigenvalues in duplicate. The super-

$$\begin{Bmatrix} \mathbf{H}^r & -\mathbf{H}^i \\ \mathbf{H}^i & \mathbf{H}^r \end{Bmatrix} \begin{Bmatrix} \mathbf{U}^r & \mathbf{U}^i \\ \mathbf{U}^i & \mathbf{U}^r \end{Bmatrix} = \begin{Bmatrix} \mathbf{U}^r & -\mathbf{U}^i \\ \mathbf{U}^i & \mathbf{U}^r \end{Bmatrix} \begin{Bmatrix} \Lambda & 0 \\ 0 & \Lambda \end{Bmatrix} \tag{7}$$

scripts refer to the real and imaginary parts. This procedure was required because our computer (RC 4000 from "Regencentralen," Copenhagen) was unable to operate with complex numbers.

The transition field positions corresponding to fixed $h\nu$ were found by an iterative procedure, giving an accuracy better than 0.1 G. $\partial\lambda_k/\partial H$ was found from

$$\begin{Bmatrix} \mathbf{U}^r & \mathbf{U}^i \\ -\mathbf{U}^i & \mathbf{U}^r \end{Bmatrix} \begin{Bmatrix} \frac{\partial}{\partial H}\mathbf{H}^r & -\frac{\partial}{\partial H}\mathbf{H}^i \\ \frac{\partial}{\partial H}\mathbf{H}^i & \frac{\partial}{\partial H}\mathbf{H}^r \end{Bmatrix} \begin{Bmatrix} \mathbf{U}^r & -\mathbf{U}^i \\ \mathbf{U}^i & \mathbf{U}^r \end{Bmatrix} =$$

$$\begin{Bmatrix} \frac{\partial}{\partial H}\Lambda & 0 \\ 0 & \frac{\partial}{\partial H}\Lambda \end{Bmatrix} \tag{8}$$

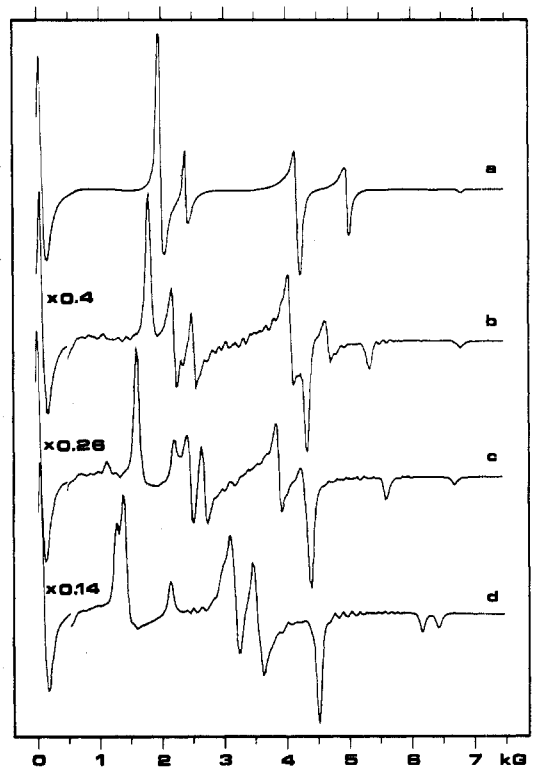

Figure 14. Computer-simulated random orientation spectra with $g_x = g_y = g_z = 1.98$, $h\nu = 0.31$ cm^{-1}, and fixed zfs $= 2\sqrt{D^2 + 3E^2} = 0.32$ cm^{-1}: (a) $E = 0$, $D = 0.16$; (b) $E = 0.01$, $D = 0.159$; (c) $E = 0.02$, $D = 0.156$; (d) $E = 0.04$, $D = 0.144$. All units are in cm^{-1}. Single molecule spectra with lorentzian line widths of 100 G were added for every following step in the polar angles Θ and Φ: (a) $\Delta\Theta = 0.5°$, $\Delta\Phi = 0°$; (b) $\Delta\Theta = 1°$, $\Delta\Phi = 3°$; (c) $\Delta\Theta = 1°$, $\Delta\Phi = 2°$; (d) $\Delta\Theta = 1°$, $\Delta\Phi = 1°$. The computer time for (d) was 30 hr with a 12 k process.

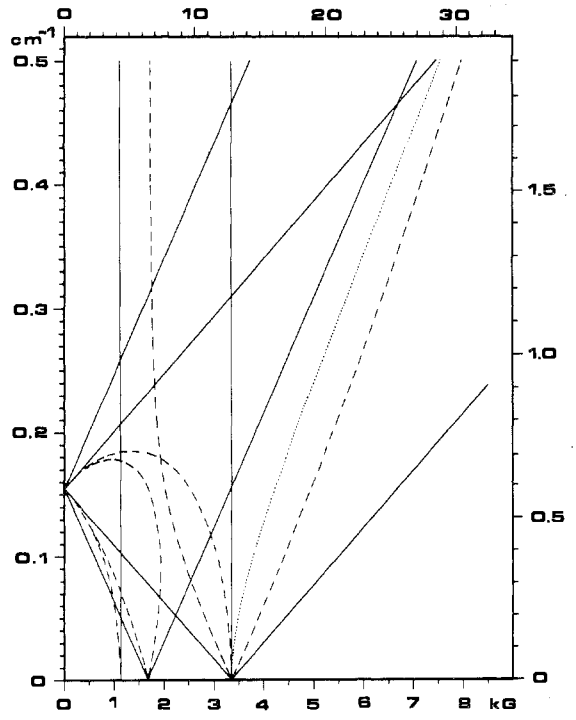

Figure 15. Resonance field positions as functions of D; $g_x = g_y = g_z = 1.98$; $E = 0$. Lower and left-hand scales correspond to $h\nu = 0.31$ cm^{-1}; the others, to 1.18 cm^{-1}: ——, $H \| z$; - - - - -, $H \| x, y$; · · · · ·, intermediate orientation.

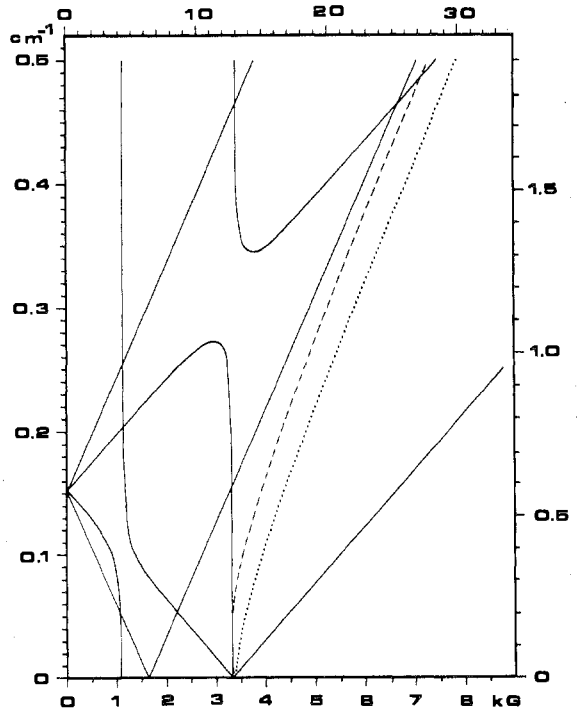

Figure 16. Resonance field positions as functions of D; $g_x = g_y = g_z = 1.98$. Lower and left-hand scales correspond to $h\nu = 0.31$ cm^{-1} and $E = 0.02$ cm^{-1}; the others, to $h\nu = 1.18$ cm^{-1} and $E = 0.076$ cm^{-1}: ——, $H \| z$; - - - - -, intermediate orientation in the zx plane; · · · · ·, intermediate orientation in the yz plane.

The relative transition probabilities are given by

$$P_{mn} \propto |\sum_{m_s m_s'} \langle \nu_m | m_s \rangle \langle m_s | \mathbf{i}\cdot\mathbf{g}\cdot\mathbf{S} | m_s' \rangle \langle m_s' | \nu_n \rangle|^2 \quad (9)$$

where the operator $\mathbf{i}\cdot\mathbf{g}\cdot\mathbf{S}$ describes the relative Zeeman perturbation from the microwave field, giving the matrix $\mathbf{H}_1$. Equation 9 in matrix notation is

$$\begin{Bmatrix} \tilde{U}^r & \tilde{U}^i \\ -\tilde{U}^i & \tilde{U}^r \end{Bmatrix} \begin{Bmatrix} H_1{}^r & -H_1{}^i \\ H_1{}^i & H_1{}^r \end{Bmatrix} \begin{Bmatrix} U^r & -U^i \\ U^i & U^r \end{Bmatrix} = \begin{Bmatrix} p_{mn}{}^r & -p_{mn}{}^i \\ p_{mn}{}^i & p_{mn}{}^r \end{Bmatrix} \quad (10)$$

where

$$P_{mn} \propto (p_{mn}{}^r)^2 + (p_{mn}{}^i)^2 \quad (11)$$

The intermediate results obtained here were found to agree with calculations performed on ruby spectra.[39]

Random orientation spectra were obtained by integrating Lorentzian functions with the positions and intensities found over three Euler angles in space. The field positions are independent of one of these. Typical results are shown in Figures 13 and 14, clearly demonstrating the importance of intermediate orientation lines. The lengthy computer calculations are condensed in the Figures 15-17. These graphs show all features to be expected in random orientation spectra of $S = {}^3/_2$ systems at X and Q bands, including intermediate orientation lines. By simple multiplications the results for other g factors and/or frequencies can be obtained. Interpolations and extrapolations can be performed linearly in the range $0 \leq E \leq 0.04$ cm^{-1}. A comparison with Figures 13 and 14 gives an impression of the intensities to be expected.

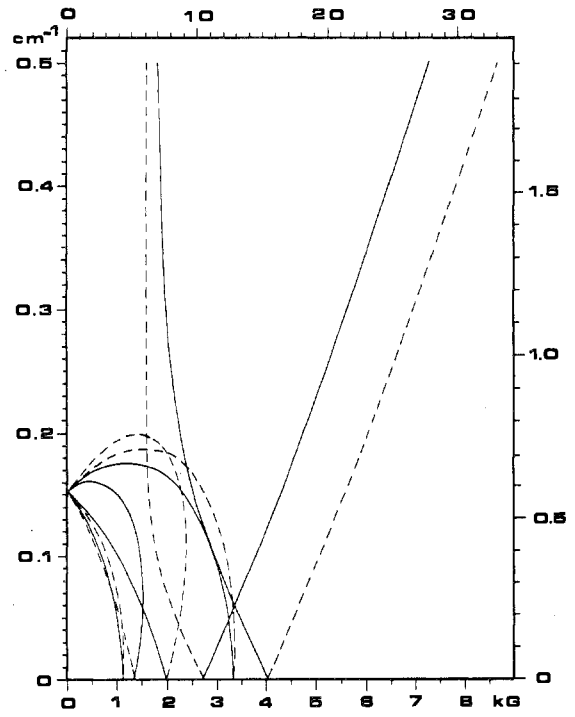

Figure 17. Resonance field positions as functions of D, for the same set of parameters as in Figure 16: ——, $H \| x$; - - - - -, $H \| y$.

Registry No. *trans*-$[Cr(py)_4I_2]^+$, 51269-30-8; *trans*-$[Cr(py)_4Br_2]^+$, 51266-52-5; *trans*-$[Cr(py)_4Cl_2]^+$, 51266-53-6; *trans*-$[Cr(py)_4F_2]^+$, 47514-84-1; *trans*-$[Cr(py)_4FBr]^+$, 51266-54-7; *trans*-$[Cr(py)_4FCl]^+$, 51266-55-8; *trans*-$[Cr(py)_4Br(H_2O)]^{2+}$, 51266-56-9; *trans*-$[Cr(py)_4Cl(H_2O)]^{2+}$, 51266-57-0; *trans*-$[Cr(py)_4F(H_2O)]^{2+}$, 51266-58-1; *trans*-$[Cr(py)_4(H_2O)_2]^{3+}$, 51266-59-2; *trans*-$[Cr(py)_4(OH)_2]^+$, 51266-60-5; *trans*-$[Cr(py)_4Cl(OH)]^+$, 51266-61-6; *trans*-$[Cr(py)_4F(OH)]^+$, 51266-62-7; *trans*-$[Cr(NH_3)_4Br_2]^+$, 51266-63-8; *trans*-$[Cr(NH_3)_4Cl_2]^+$, 22452-49-9; *trans*-$[Cr(NH_3)_4F_2]^+$, 31253-66-4; *trans*-$[Cr(NH_3)_4FBr]^+$, 51266-64-9; *trans*-$[Cr(NH_3)_4F(H_2O)]^{2+}$, 40029-19-4; *trans*-$[Cr(NH_3)_4(H_2O)_2]^{3+}$, 36834-73-8; *trans*-$[Cr(NH_3)_4(OH)_2]^+$, 51266-65-0; *trans*-$[Cr(NH_3)_4(NCS)_2]^+$, 51266-66-1; *trans*-$[Cr(NH_3)_4Br(ONO)]^+$, 51266-67-2; pyridine, 110-86-1; *trans*-$[Rh(py)_4Br_2]Br$, 14267-74-4.

(39) J. H. Mackey, M. Kopp, E. C. Tynan, and T. F. Yen in "Electron Spin Resonance of Metal Complexes," T. F. Yen, Ed., Adam Hilger, London, 1969, p 33.